

Complex spatial structure of ion yield arising from high-intensity multiphoton ionization

T. J. McIlrath

Institute for Physical Science and Technology, University of Maryland, College Park, Maryland 20742

R. R. Freeman

AT&T Bell Laboratories, Murray Hill, New Jersey 07974

W. E. Cooke

Department of Physics, University of Southern California, Los Angeles, California 90007

L. D. van Woerkom

AT&T Bell Laboratories, Murray Hill, New Jersey 07974

(Received 7 February 1989)

Recent measurements of the electron-energy distribution for high-intensity short-pulse multiphoton ionization in xenon have yielded a spectrum unexpectedly rich in well-resolved peaks, apparently arising from optical Stark shifts of atomic levels into resonance with harmonics of the ionizing laser. Here we show that such a resonance structure is, quite generally, accompanied by a surprisingly complex *spatial* structure of the total ionization yield. We predict this spatial structure to arise in a wide variety of multiphoton experiments.

In a recent paper, Freeman *et al.*¹ reported the observation of an unexpected fine structure in the electron-energy spectrum for short-pulse high-intensity multiphoton ionization in xenon. This result, subsequently confirmed in xenon by other researchers² and also recently observed by us in krypton, argon, and neon, is thought to be due to optical Stark shifts of atomic levels during the course of the intense laser pulse. Here we show that when such a structure appears in the energy spectrum, the resulting ionization yield is necessarily distributed spatially throughout the interaction volume in a complex, inhomogeneous manner. We demonstrate that the form of this spatial structure can be derived directly from that of the fine structure in the electron-energy spectrum.

In an intense optical field with peak intensity I and frequency ω , the ionization threshold (I_{th}) increases its energy relative to the ground state by the ponderomotive energy,³ viz., $U_p(I) = 2\pi e^2 I / m_e c \omega^2$. For long-pulse excitation this threshold increase is effectively masked in the photoelectron spectra,⁴ but under the conditions of short-pulse excitation, the photoelectrons all arrive at the detector with their energy reduced^{1,5} by $U_p(I)$, where I is the intensity at the moment of photoionization for each electron. The high-lying Rydberg states of atoms or molecules increase in energy relative to the ground state by approximately⁶ $U_p(I)$, opening up the possibility that they will shift into resonance with the m th harmonic of the laser frequency sometime during the pulse.^{7,8} States that can enhance the multiphoton ionization rate must have a zero-field energy that is less than $m\hbar\omega$ above the ground state and have the appropriate parity. The occurrence of such a resonance increases the ionization yield at a specific photoemission energy.¹ Figure 1 shows a portion of the record of electron kinetic energies obtained in high intensity ($\leq 7 \times 10^{13}$ W/cm²) multiphoton

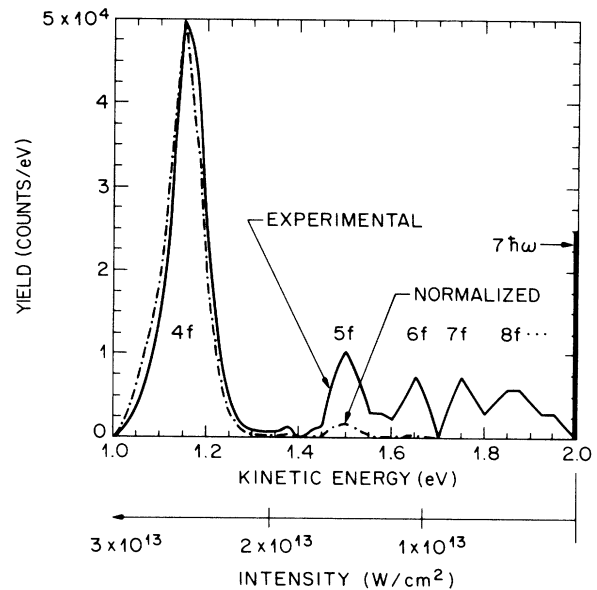


FIG. 1. A portion of the experimental record of electron kinetic energies $N(E)$ obtained in high-intensity ($\leq 7 \times 10^{13}$ W/cm²) multiphoton photoemission of xenon for a laser at 616 nm with a pulse width of ≈ 250 fsec. Because of the connection between the ponderomotive potential, the high intensity light, and the shift of the atomic ionization potential, the abscissa is also labeled with the intensity of light experienced by each atom. The "normalized" spectrum is obtained by dividing the experimental spectrum at each energy by a value proportional to the effective spatial volume which can contribute photoelectrons at that energy [Eq. (2)].

photoemission of xenon for a laser at 616 nm with a pulse width of ≈ 250 fsec. At 616 nm, xenon requires seven photons to ionize the ground state, and the sixth harmonic ($6\hbar\omega$) lies just 0.05 eV below the (zero-field) ionization threshold I_{th} . This relative positioning in energy of $6\hbar\omega$ and the xenon ionization threshold places the sixth harmonic just above the unshifted energy positions of a large family of xenon excited states. The position labeled $7\hbar\omega$ is the energy that electrons would have if photoemitted by seven-photon ionization without a ponderomotive shift.

The resonance structure in the kinetic energy spectrum in Fig. (1) is uniquely related to the specific intensities required to shift the excited states into six-photon resonance with the laser.¹ This intensity is the same for all atoms in the interaction volume; thus the abscissa on Fig. 1 may be relabeled according to the intensity I , with the conversion factor derived from the ponderomotive potential ($I(W/cm^2) = [(2.0 - E)/(0.37 \text{ eV})] \times 10^{13}$ at 616 nm). The states are labeled in Fig. 1 by assuming their optical Stark shifts to be approximately ponderomotive.

The ponderomotive shift at any position (r, z) and time t within the ionization pulse is directly proportional to the local intensity⁸ $I(r, z, t)$; at the focus ($z=0$), $I(r, t) = I_0 \exp[-(r/r_0)^2 - (t/\tau)^2]$. If the intensity required to shift one of the f states into six-photon resonance is I_R , where $I_R < I_0$, electrons with energy E_R will be produced at the temporal peak of the pulse (i.e., $t=0$) from atoms in a narrow spatial band centered at $r_1 = r_0 [\ln(I_0/I_R)]^{1/2}$. However, electrons with the same energy E_R from the same f state are also produced by different atoms whose radial positions satisfy $r < r_1$. These atoms also produce their electrons at $I = I_R$, but at times other than $t=0$: once when the intensity passes through I_R on the leading edge of the pulse and again on the falling edge.

The ionization rate is a convoluted function of time and space.⁹ However, the assumption that high-intensity photoemission arises primarily from level crossings yields a significant simplification: Because each atom undergoes an m -photon resonance for a given state at precisely the same intensity, regardless of the spatial location of the atom, the ionization probability can vary from atom to atom only because the amount of time each atom experiences that intensity depends upon its location in the beam focus. This time is greatest for those atoms located where the resonance intensity I_R occurs at the peak in the local intensity; i.e., where $I(t) = I_R \exp[-(t/\tau)^2]$. At these points the resonance time interval is $t \approx \tau$; however, at spatial points where $I(t) = I_p \exp[-(t/\tau)^2]$ and $I_p > I_R$, resonance occurs only on the leading and falling edge of the pulse, and the time interval for resonance is much less than τ . *It is this spatial variation in "resonance time" that produces a nonmonotonic variation of total ionization with radius.* Here we outline a quantitative model of the spatial dependence of the ionization probability based upon Landau-Zener curve crossing theory¹⁰ extended¹¹ to account for curve crossings having not only the usual linear dependence on time (as on the steep edges of the pulse), but quadratic as well (as near the top of the pulse). The full derivation is given elsewhere.¹¹

Consider two states: State 1 is the excited Rydberg level of the atom, and state 2, assumed to lie above state 1, is the ground state dressed by m photons. These levels are initially separated in energy by $\hbar\omega_R$, but because of the optical Stark shift of state 1, the separation $\hbar\omega$ decreases with increasing laser intensity according to $\omega = \omega_R(1 - I/I_R)$, where I_R is the intensity for the levels to cross (i.e., "resonance"). The first and second derivatives of the energy separation are used to parametrize the level separation with time. For a laser beam with a Gaussian distribution in time and for $I = I_R$, $|\partial\omega/\partial t| = (2\omega_R/\tau)[\ln(I_p/I_R)]^{1/2}$. If $I_R = I_p$, so that the resonance occurs at the peak of the local beam intensity where $\partial\omega/\partial t = 0$, then $|\partial^2\omega/\partial t^2| = 2\omega_R/\tau$ [ignoring terms of order $(t/\tau)^2$].

Conventional Landau-Zener theory for a curve crossing linear in time computes the probability for a transition from the ground (state 2) to the excited state (state 1) to be $P = 1 - \exp(-p)$, where $p = 2\pi V^2 \tau_c^2$ with $\hbar V$ equal to the interaction strength [proportional to $(I_R)^m$ in this instance] and $\tau_c^2 = |\partial\omega/\partial t|^{-1}$. (Assuming that the ionization cross section of state 1 is sufficiently large that no population is coherently returned to the ground state.) When $I_p = I_R$, $\partial\omega/\partial t \approx 0$, τ_c is dominated by the second-order derivative and can be shown¹¹ by direct integration to be $\tau_c^2 = \alpha^2 |\partial^2\omega/\partial t^2|^{-2/3}$, where $\alpha^2 = (1/2\pi)(\frac{1}{3})^{1/3} [\Gamma(\frac{1}{3})]^2$. Adding the linear and quadratic rates in quadrature, and assuming no coherence in the excitation, yields the total ionization probability from resonance R at any spatial location to be

$$P = \frac{N'(r)}{N_0} [1 - \exp(-p)], \quad (1)$$

$$p = p(r, z, \omega_R) = 2\pi V_R^2 (\tau/\omega_R) \frac{\epsilon}{1 + \epsilon [\ln(I_p/I_R)]^{1/2}},$$

where $\epsilon = \Gamma^2(1/3)(\omega_R \tau/3)^{1/3}/2\pi = 0.79(\omega_R \tau)^{1/3}$. Here $I_p = I_p(r)$ is the peak intensity at $t=0$ at position (r, z) in the beam; at $z=0$, I_p and r are related to I_0 , the peak intensity at $r=0$, and r_0 , the spot size at the focus by $r = r_0 [\ln(I_0/I_p)]^{1/2}$. $N'(r)$, the ground-state density remaining after the ionization due to all j atomic resonances requiring less intensity than I_R , is related to N_0 , the initial ground-state density, by $N'(r) = N_0 \exp(-\sum_{i=1}^j p_i)$.

Under conditions far from saturation, $p \ll 1$, yielding $P \approx p$, but Eq. (1) correctly predicts the general case. We have elsewhere¹² considered explicitly how the spatial structure is distorted by saturation. For the purposes of this paper it is sufficient to note that short-pulse multiphoton ionization measurements provide an empirical monitor of the role of saturation: the quality of the structure in the photoelectron energy spectrum. If there were saturation, the structure at the lower kinetic energies, corresponding to levels requiring more intensity to undergo resonance (and thus later in the pulse for all r), would be absent or seriously attenuated. However, none of the data we have taken in short-pulse multiphoton ionization measurements shows any sign of saturation for any resonance. Indeed, the ratio of signal strength of the $4f$ to $5f$

resonances in the volume normalized spectra in Fig. 1 is very nearly what one would expect from a ratio of resonance intensities raised to the sixth power. For these reasons our further discussion assumes the weak ionization limit, although we emphasize that Eq. (1) is quite general and applies to arbitrary ionization probabilities as well.

The total ionization contributed to the photoemission spectrum $N(E)$ from resonance R is obtained by summing contributions from all points in the volume. That is, integrating $N_0 P = N_0 p$ over all space, we find (after the explicit radial integration)

$$N(\omega_R) = 8\pi^2 N_0 V_R^2 \left[\frac{\tau}{\omega_R} \right] \times \int_0^{Z_m} \left[(1+z^2) \left(u - \frac{1}{\epsilon} \ln(1+\epsilon u) \right) \right] dz, \quad (2)$$

where

$$u = \left[\ln \frac{I_0}{I_R(1+z^2)} \right]^{1/2}, \quad Z_m = \sqrt{I_0/I_R - 1}.$$

Equations (1) and (2) allow the calculation of both the spatial and energy distribution of a high-intensity multiphoton experiment given a list of the atomic energy levels and the m -photon transition strengths: First calculate the spatial distribution from Eq. (1), then weight the contribution of each resonance in the energy distribution by computing its effective volume [Eq. (2)].

To calculate the spatial distribution from an experimental record of the energy spectrum $N(E)$, (i) deconvolute the energy response function of the electron-energy analyzer from the recorded data, (ii) determine the contribution of each E_R contained in $N(E)$ to the spatial yield by first normalizing $N(E)$ by $N(\omega_R)$ (we have shown the application of this normalization to the experimental data in Fig. 1; the effective volume of resonances with small values of I_R , e.g., $6f, 7f, \dots$, is so large that it contributes significantly to the experimental photoemission spectrum, even though its intrinsic strength, shown in the normalized spectrum, is negligible), (iii) apply Eq. (1) to determine the total ionization at (r, z) , that is,

$$N(r, z) = \int [N(E_R) N_0 p(r, z, \omega_R) / N(\omega_R)] dE_R.$$

We have applied this procedure to the data in Fig. 1. Figure 2 shows the results: The peak intensity in the beam is taken to be 7×10^{13} W/cm². The Gaussian beam profile and the distribution of photoemitted electrons assuming truly nonresonant, seven-photon multiphoton ionization are also shown. Note that while the position of the peak in the nonresonant distribution is independent of I_0 , that of the resonant ionization scales as $(\ln I_0)^{1/2}$. The complex spatial structure introduced in

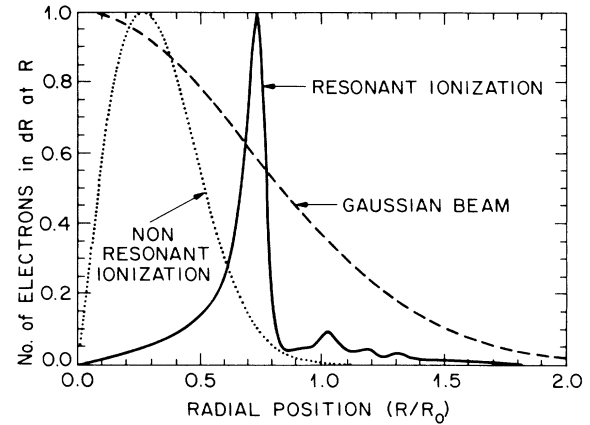


FIG. 2. The resultant *spatial* distribution at $z=0$ of total ionization yield calculated from the *energy* spectrum shown in Fig. 1 for an intensity of 7×10^{13} W/cm². Also shown is the ionization yield assuming conventional seven-order "nonresonant" ionization. The position of the peak of the nonresonant distribution is independent of I_0 , while that for resonant ionization scales as $(\ln I_0)^{1/2}$.

Fig. 2 by the excited atomic states is dramatic.¹³

The complex spatial distribution of ionization introduced by resonances is expected to influence several kinds of high-intensity multiphoton experiments. In sequential ionization,^{6,14} for example, the rising laser pulse first ionizes the neutral atom and then, at higher intensities, produces higher stages of ionization in a sequential manner. These experiments are usually analyzed by assuming that at saturation the resulting ions are produced primarily on axis, with a monotonically decreasing density with radius. These ions are then presumed to have been exposed to higher intensities where they nonresonantly ionize further. In contrast, this paper demonstrates that the ionization density for any stage will not necessarily fall off monotonically with radius, but may be instead concentrated in the regions of "spatial resonances." In general, the spatial resonances for one stage of ionization will not match up with the spatial regions of resonance for the succeeding ionization stage. Although saturation due to long laser pulse lengths or very large atomic transition strengths may limit the effects of this mismatch, we expect the complex ionization distributions to play a significant role in inhibiting multiple ionization; however, their effects can be explicitly calculated using the procedure outlined here.

The authors wish to thank A. Szöke for several important discussions at the inception of this work, P. H. Bucksbaum for a critical reading of the manuscript, J. Nodvik for deriving the $\Gamma(\frac{1}{3})$ factor, and S. Davey for technical help. One of us (W.E.C.) was supported by National Science Foundation (NSF) Grant No. PHY85-0085 and another (T.J.M.) by NSF Grant No. CPE-84-179333.

¹R. R. Freeman, P. H. Bucksbaum, H. Milchberg, S. Darack, D. Schumacher, and M. E. Geusic, Phys. Rev. Lett. **59**, 1092 (1987).

²H. G. Muller, H. B. van Linden van den Heuvell, P. Agostini,

G. Petite, A. Antonetti, M. Franco, and A. Migus, Phys. Rev. Lett. **60**, 565 (1988).

³T. J. McIlrath, P. H. Bucksbaum, R. R. Freeman, and M. Bashkansky, Phys. Rev. A **35**, 4611 (1987).

- ⁴H. G. Muller, A. Tip and M. J. van der Wiel, *J. Phys. B* **16**, L679 (1983); T. W. B. Kibble, *Phys. Rev.* **150**, 1060 (1966).
- ⁵M. Crance, *J. Phys. B* **21**, 2697 (1988); T. S. Luk, T. Graber, H. Jara, U. Johann, K. Boyer, and C. K. Rhodes, *J. Opt. Soc. Am. B* **4**, 847 (1987); P. Agostini, J. Kupersztych, L. A. Lompre, G. Petite, and F. Yergeau, *Phys. Rev. A* **36**, 4111 (1987); R. R. Freeman, P. H. Bucksbaum, and T. J. McIlrath, *IEEE J. Quantum Electron.* **24**, 1461 (1988).
- ⁶L. Pan, L. Armstrong, and J. H. Eberly, *J. Opt. Soc. Am. B* **3**, 1319 (1986); P. Avan, C. Cohen-Tannoudji, J. Dupont-Roc, and C. Fabre, *J. Phys. (Paris)* **37**, 993 (1976); M. D. Perry, A. Szoke, O. L. Landen, and E. M. Campbell, *Phys. Rev. Lett.* **60**, 1270 (1988).
- ⁷M. Crance, *J. Phys. B* **14**, 4301 (1981); O. L. Landen, M. Perry, and E. M. Campbell, *Phys. Rev. Lett.* **59**, 2558 (1987).
- ⁸Here we are interested only in deriving the spatial distribution at $z=0$. The method is quite general to all other points within the volume, only a more mathematically tedious expression for the Gaussian beam is required for $z \neq 0$; see A. Yariv, *Quantum Electrons*, 2nd ed. (Wiley, New York, 1975), p. 110.
- ⁹M. D. Perry and O. L. Landen, *Phys. Rev. A* **38**, 2815 (1988).
- ¹⁰A. Szöke, *J. Phys. B* **21**, L125 (1988); M. Crance, *ibid.* **21**, 1987 (1988).
- ¹¹W. E. Cooke, R. R. Freeman, T. J. McIlrath, and L. D. van Woerkom (unpublished). See also M. V. Fedorov and A. E. Kazakov, *Prog. Quant. Electron.* **13**, 1 (1989).
- ¹²L. D. van Woerkom, R. R. Freeman, W. E. Cooke, and T. J. McIlrath, *J. Mod. Opt.* **36**, 817 (1989).
- ¹³If the atom is exposed to even high intensities, there will be the possibility of additional level crossings, corresponding to $m+2, m+4, \dots, m+2n$ photons.
- ¹⁴A. L'Huillier, L. A. Lompre, G. Mainfray, and C. Manus, *Phys. Rev. Lett.* **48**, 1814 (1982); *Phys. Rev. A* **27**, 2503 (1983); *J. Phys. B* **16**, 1363 (1983); T. S. Luk, U. Johann, H. Egger, H. Pummer, and C. K. Rhodes, *Phys. Rev. A* **32**, 214 (1985).